

Dynamics of Raindrops: A Comprehensive Analysis of Terminal Velocity Across Different Reynolds Numbers

Reece Iriye

November 1, 2023

1: Introduction

A critical area of research in understanding the dynamics of raindrops is the study of their terminal velocities—the constant speed achieved by a falling raindrop when the force of gravity is balanced by the resistance of air. This balance is governed by a multitude of factors, including the raindrop's size, shape, and the surrounding air's properties. Central to this analysis is the concept of the Reynolds number (Re), a dimensionless quantity that characterizes the nature of flow around the raindrop. The Reynolds number incorporates density, velocity, size, and viscosity all into a single value, thus playing a pivotal role in determining the drag force experienced by the raindrop and, consequently, its terminal velocity.

This paper presents a comprehensive examination of the terminal velocities of raindrops, addressing both small and large droplets within different Reynolds number domains. By investigating a multitude of approaches, the study aims to provide a thorough understanding of raindrop dynamics. The investigation begins with the perfect sphere assumption, a fundamental hypothesis in fluid dynamics and aerodynamics, and progressively dives deeper into different models spanning different domains that account for the realities of raindrop descent through the atmosphere. Through this analysis, the paper aims to compare simplified theoretical models and models trained off of existing raindrop data. It also seeks to explore these models' performance across various domains, offering valuable insights about the dynamics of raindrops as a whole.

2: Raindrop Reynolds Number and the Perfect Sphere Assumption

The Reynolds number (Re) is expressed by the formula in **Equation (1)**, where ρ_{air} represents the density of the air, v represents the velocity of the raindrop, l represents the characteristic length of the raindrop, and μ_{air} represents the viscosity of the air.

$$\text{Re} = \frac{\rho_{air} v l}{\mu_{air}} \quad (1)$$

The National Institute of Standards and Technology (NIST) declared the standard pressure and temperature to be 101.325 kPa and 20°C (68°F) respectively [1]. They declared these values to be the norm in 1931, and several studies have incorporated these standards into their studies ever since. For the purposes of this paper honing in on raindrop behavior, I will adopt these standards for identifying the density and viscosity of air as constants. Using these standards, the density of air can be represented as $\rho_{air} \approx 1.2041 \text{ kg/m}^3$, and the viscosity of air can be represented as $\mu_{air} \approx 1.81 \times 10^{-5} \text{ Pa}\cdot\text{s}$ [2,3].

The characteristic length l of an object plays a crucial role in determining its interaction with the surrounding atmosphere. For raindrops, this characteristic length is often assumed to be the diameter of the droplet, under the assumption that the raindrop is a perfect sphere [4]. This assumption simplifies the complex interaction between the raindrop and the air through which it falls, allowing for more straightforward mathematical modeling and analysis that I will incorporate throughout the rest of this paper. The spherical assumption is particularly strong in modeling relatively smaller raindrops, where the shape is more likely to resemble a perfect sphere due to the surface tension of water.

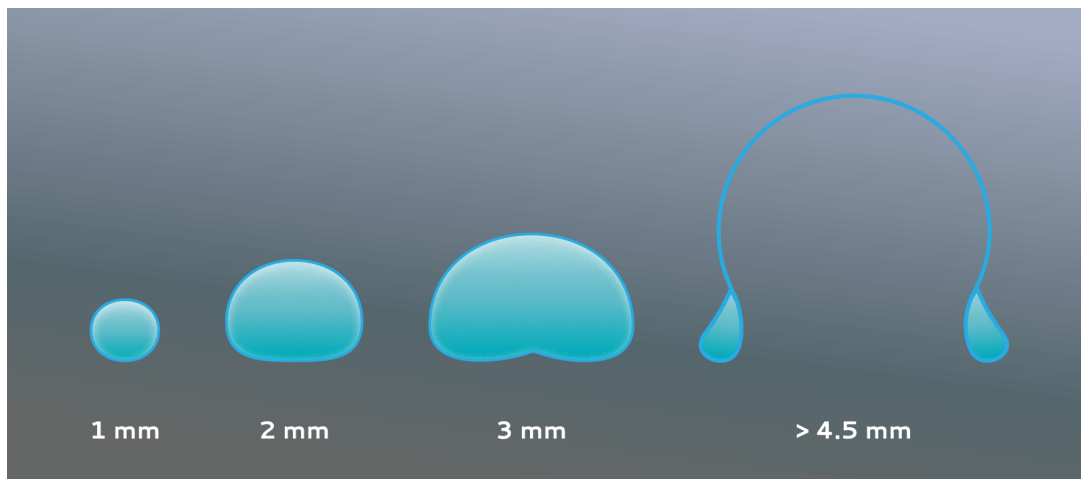


Figure 1: *Approximate Rain Drop Lengths at Various Characteristic Lengths* [5]

The assumption of a perfect sphere, however, has its limitations, especially when considering larger raindrops. As the size of a raindrop increases, the forces acting on it cause deviations from the ideal spherical shape, as seen in **Figure 1**. Contrary to the common misconception of a teardrop shape, larger raindrops tend to adopt a more "bowed out" form with the bottom surface becoming increasingly flattened or even concave. This deviation from an ideal sphere can lead to significant errors in predictions made using models that rely on the perfect sphere assumption. The impact of this discrepancy could appear in my calculation of drag force and terminal velocity, as these rely heavily on the shape and size of the raindrop. Thus, while the spherical assumption is a useful starting point for understanding raindrop dynamics, especially for smaller droplets, it becomes increasingly inaccurate as the size of the raindrop grows. Recognizing and accounting for these limitations is crucial in developing more accurate

and comprehensive models for raindrop behavior, and it's also helpful in understanding the advantages and pitfalls of my models that I will present throughout this paper. While none of the raindrop data from Gunn and Kinzer exceeds 3mm [6], a somewhat significant deviation from the ideal spherical shape assumption occurs in reality nonetheless.

3: Modeling Terminal Velocities for Small Rain Drops

The significance of developing a simple model tailored for small raindrops where $Re \ll 1$ that respects the dimension quantities of each variable and parameter cannot be overstated. In this domain, the viscous forces play a dominant role [8]. This is a huge difference in contrast to larger droplets where $Re \gg 1$ and inertial effects become significant. By focusing on this low Reynolds number domain, I target a range where the spherical assumption is most appropriate as seen in **Figure 1**, and the drag force can be adequately described by the linear relationship in **Equation (2)** where k_1 represents the drag coefficient.

$$F_D = k_1 \mu_{air} v d \quad (2)$$

$$F_g = \frac{4}{3} \pi r^3 \rho_{water} g \quad (3)$$

In modeling terminal velocity with **Equation (2)** and **Equation (3)**, I can conclude that these raindrops are in an equilibrium state. Because of this equilibrium, the magnitudes of these forces are then equal to 0 N, which means that force balance equations can be used to solve v in terms of d .

$$v = \frac{\pi \rho_{water} g}{6 k_1 \mu_{air}} \cdot d^2 \quad (4)$$

By acknowledging that the radius of each droplet is equivalent to half of its diameter $r = d/2$, and by setting F_D and F_g equal to one another and solving for v , we find **Equation (4)**. By fitting this equation to the raindrops where $Re \ll 1$, I find that $k_1 \approx 9.994$.

This fitted value for k_1 is intriguing, as it relatively deviates by 6.039% from the theoretical expectation based on Stokes' law [7], which suggests that the drag coefficient $k_1 = 3\pi \approx 9.425$. This deviation is indicative of the complex interplay between theoretical models and real-world observations. Theoretical models often rely on idealized assumptions and conditions, such as the perfect spherical shape of raindrops and uniformity in environmental conditions. The NIST values I used to pre-label ρ_{air} and μ_{air} , for example, are likely incorrect. In contrast, the empirical approach captures some nuances and variations inherent in natural phenomena that Stokes' Law didn't capture due to its simplicity. This is particularly true for raindrops, whose behavior can be influenced by factors such as air density fluctuations, wind, and even the presence of impurities in the water.

Figure 2 illustrates the comparison between the fitted polynomial model and the theoretically derived polynomial from Stokes' Law for extremely low Reynolds numbers. The stronger fit

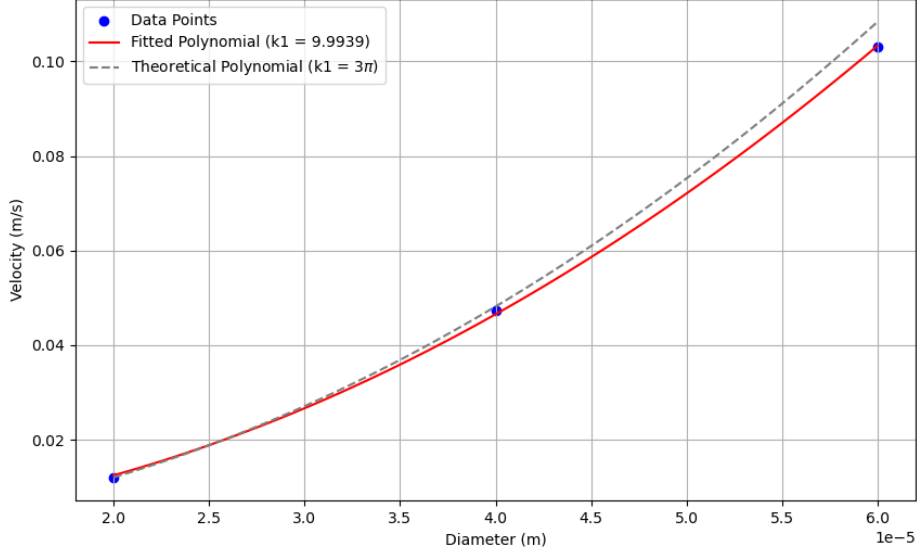


Figure 2: *Fitted Polynomial vs. Theoretically Derived Polynomial for $Re \ll 1$*

of the data-driven model reveals its capability to accommodate the subtleties that are often overlooked in theoretical formulations. The data-driven model does not deviate as strongly from the true terminal velocities as the diameter increases in the $Re \ll 1$ domain.

4: Modeling Terminal Velocities for Large Rain Drops

Transitioning from the realm of smaller raindrops, where viscous forces dominate, to larger ones, where inertial effects become significant, presents a new set of challenges and opportunities. In this domain, characterized by $Re \gg 1$, the drag force experienced by the raindrops is predominantly influenced by inertial rather than viscous effects. This shift necessitates a different modeling approach. To accommodate these changes, the drag force is now assumed to satisfy the relation in **Equation (5)**, where k_2 represents a new drag coefficient for this regime.

$$F_D = k_2 \rho_{air} v^2 d^2 \quad (5)$$

In the case of terminal velocity, this drag force can be set equal to the gravitational force, as described in **Equation (3)**, yielding a new expression for the squared terminal velocity of larger raindrops expressed in **Equation (6)**.

$$v^2 = \frac{\pi \rho_{water} g}{6 k_2 \rho_{air}} \cdot d \quad (6)$$

Fitting this model to the three rain droplets in the dataset where $Re \gg 1$, I find that $k_2 \approx 0.223$. This value differs heavily from the theoretical expectation derived from the general drag equation for a sphere of higher Reynolds numbers, $F_D = \frac{1}{2} C_D \rho v^2 A$, where the cross-sectional

area $A = \pi r^2$ under the assumption of a raindrop being a perfect sphere [8]. In this context, $k_2 = \frac{C_D \pi}{8} \approx 0.185$ for a smooth sphere where $C_D \approx 0.47$. The discrepancy of 20.67% between the theoretical value for k_2 and the fitted k_2 reflects a dramatic difference in the derivative of this polynomial. This difference becomes increasingly impact in the domain of $Re \gg 1$, where the diameter is significantly larger, leading to a greater deviation of the theoretical model from the actual data, as there exists no bias term in this equation and the diameter is further in this context from 0 m than in the $Re \ll 1$ regime.

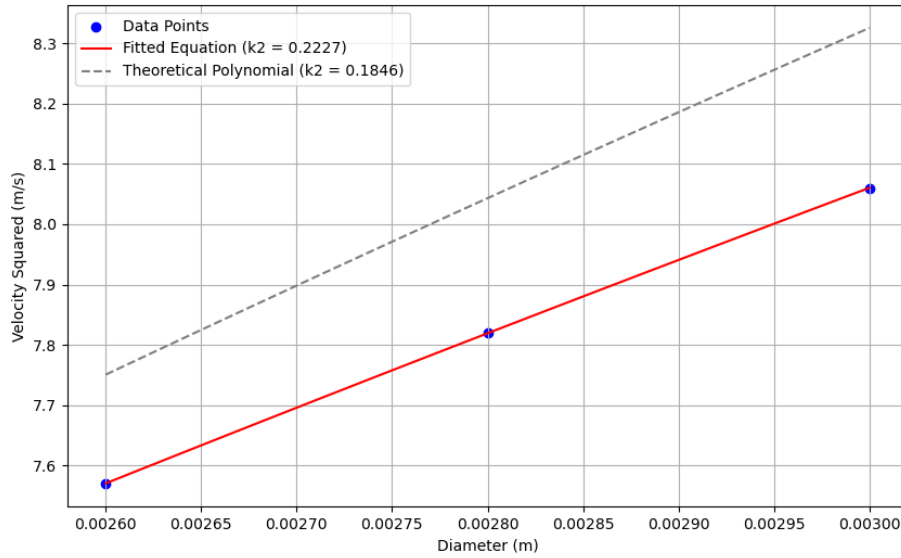


Figure 3: *Fitted Polynomial vs. Theoretically Derived Polynomial for $Re \gg 1$*

Figure 3 showcases the comparison between the fitted polynomial model and the theoretically derived polynomial for high Reynolds numbers. The superior fit of the data-driven model, particularly in this high Reynolds number range, can be largely attributed to the divergence from the spherical shape assumption in reality, as larger raindrops tend to deviate more significantly from a spherical form. This mismatch in shape becomes more pronounced in raindrops within the 2 – 3 mm range as seen in **Figure 1**, showcasing the limitations of the spherical assumption and its impact on terminal velocity predictions.

Furthermore, the potential inaccuracies in environmental variables such as ρ_{air} and μ_{air} , which were assumed based on standard atmospheric conditions, still exist in this context. My assumptions for these values might not precisely reflect the actual conditions in which these raindrops fall. This divergence from theoretical assumptions to real-world scenarios highlights the importance and effectiveness of an empirical approach, especially in the study of larger raindrops where complexities and deviations from ideal models are more pronounced.

5: Numerical Alternative for Both Small and Large Raindrops

While **Equation (4)** and **Equation 6** serve as strong models within their respective Reynolds number domains for predicting raindrop terminal velocity, I would prefer to pursue a comprehensive model capable of accurately predicting terminal velocities across all domains of Reynolds numbers. Thus, my goal is to employ a model that not only addresses the distinct characteristics of both small and large raindrops but also provides consistent predictions across the entire range of Reynolds numbers—simultaneously while being able to assume the raindrop is a perfect sphere when it does not in reality. This ambition leads me to explore a numerical approach approached by Polezav et al., diverging from the region-specific models previously discussed [9].

$$C_d \approx \frac{24}{Re} + \frac{3e^{-0.002Re}}{(Re)^{0.4}} + 0.47 \quad (7)$$

This equation serves as a bridge, capturing the intermediary patterns that pop up between low and high Reynolds number regimes [9]. By applying the Newton-Raphson method to **Equation (7)**, I can create a model that aims to directly calculate terminal velocities, accounting for the varying dynamics of different-sized raindrops.

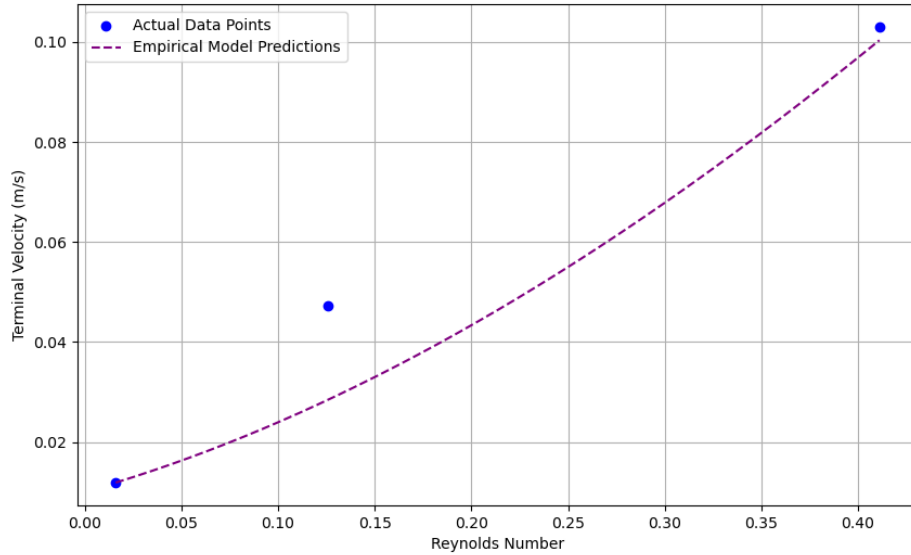


Figure 4: *Numerical Model Fit to Collected Data for $Re \ll 1$*

Figure 4 displays the performance of this numerical model against the collected data for smaller raindrops ($Re \ll 1$). The model approximates the endpoints well, but it struggles to capture the pattern in between, particularly in the mid-range of the dataset. While the data appears to curve upwards from the initial point to the 3rd point, the model approximates the region in between by curving upwards as the Reynolds number increases. This discrepancy reveals the model's limitation in accurately reflecting the subtleties of smaller raindrop dynamics where viscous forces are more prominent.

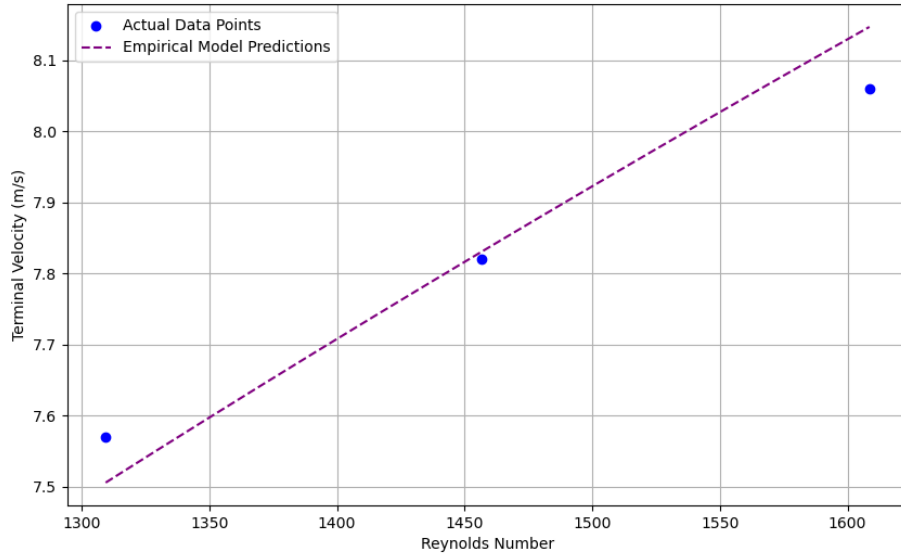


Figure 5: *Numerical Model Fit to Collected Data for $Re \gg 1$*

Figure 5 illustrates the model's performance for larger raindrops ($Re \gg 1$). In this context, the model predicts the terminal velocity of the raindrop represented by the second highest Reynolds number well, but it overshoots the point after it and undershoots the point behind it. This pattern suggests that the model still falls short of capturing the complete spectrum of behaviors.

Upon comparison, it can be concluded that the region-specific models, developed based on **Equation (4)** for small raindrops ($Re \ll 1$) and **Equation (6)** for large ones ($Re \gg 1$), outperform the numerical model in their respective domains. These models, tailored to the specific characteristics of each regime, demonstrate a more precise alignment with the actual data. Specifically within these extreme regions, the numerical model fails to perform as well as the region-specific models in predicting terminal velocity in their respective domains.

6: Comparing All Models Across a Broader Domain

While the region-specific models excel at predicting terminal velocity within their respective domains, it is essential to evaluate how the models developed so far perform across the entire domain of Reynolds numbers. This broader perspective is particularly important given the intricacies involved in raindrop dynamics, where different forces dominate in different regimes. The numerical model in **Equation (7)**, developed with the aim of capturing general intermediary patterns based on varying Reynolds numbers, is put to test against the region-specific models developed for extreme Reynolds number domains.

Figure 6 presents a log-log comparison of the fitted models for small and large Reynolds numbers against the numerical model across the entire domain of raindrop sizes. While

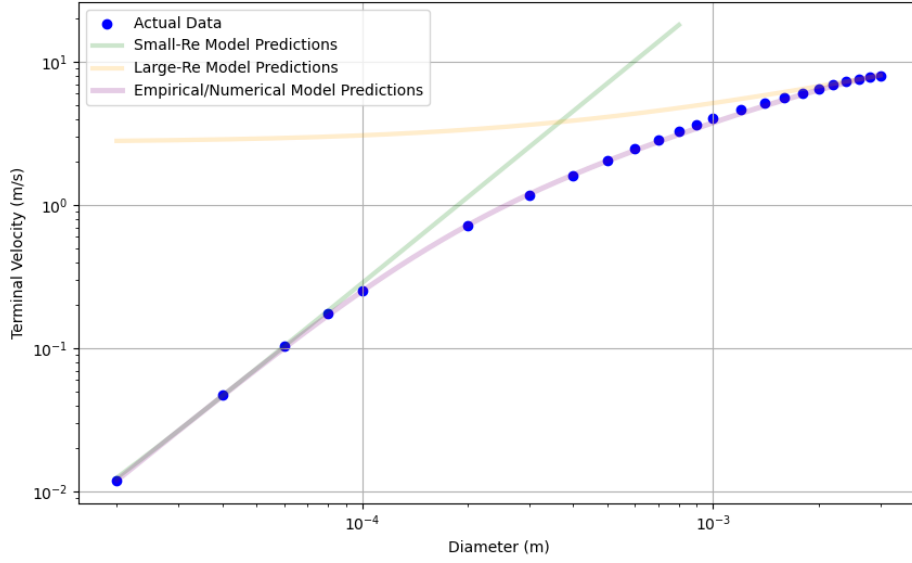


Figure 6: *Comparing the Fitted and Numerical Models Across the Entire Domain*

expected, the numerical model remarkably exhibits a stronger performance in the intermediary areas, seamlessly capturing the overarching trends demonstrated by the raindrop data. It successfully bridges the gap between the low and high Reynolds number domains, providing a more holistic representation of raindrop dynamics—specifically the relationship between droplet’s diameter and terminal velocity.

In the domain where $Re \ll 1$, **Equation (4)** excels within its designated range. However, as the Reynolds number begins to exceed certain thresholds (around 0.4), its performance noticeably diminishes. This failure of the model as the Reynolds number exits the $Re \ll 1$ region is evidenced by the model’s increasing deviation from the actual data trends, a consequence of its limited scope and inability to adapt to the changing dynamics as the Reynolds number approaches the intermediary domain.

Similarly, **Equation (6)**, which is designed for large raindrops ($Re \gg 1$), shows a decline in accuracy as the Reynolds number decreases below 1000. Its predictions, while consistent within its intended range, fail to adapt to the subtler variations observed in smaller raindrops, resulting in a somewhat linear trend in the log-log plot that doesn’t quite align with the actual data.

The numerical model not only aligns with the observed data in the intermediary range but also maintains a strong, flexible performance across the entire domain. It adapts dynamically to the changing influences of viscous and inertial forces, thus providing a more accurate and encompassing representation of raindrop behavior across different sizes and conditions.

7: Conclusion

Using region-specific models to predict raindrop dynamics across a variety of diameters is difficult, especially considering how the relationship between diameter and terminal velocity fluctuates across varying Reynolds numbers. In evaluating these models, it became increasingly apparent that capturing this inherent relationship that raindrops hold demanded a more comprehensive approach.

The numerical model presented in **Equation (7)** emerged as a significant breakthrough in its ability to track raindrop dynamics trends. Unlike the region-specific models, which excelled in either the low Reynolds number domain ($Re \ll 1$) or the high Reynolds number domain ($Re \gg 1$), the numerical model demonstrated an exceptional ability to capture the underlying trend of raindrop dynamics across the entire spectrum of Reynolds numbers. This performance is illustrated in **Figure 6**, where the numerical model adeptly bridges the gap between the varying dynamics of different-sized raindrops, providing an overall representation of their behavior.

This achievement is particularly noteworthy, especially given how difficult it is to model raindrop dynamics. As raindrops increase in size, they experience not only a shift in the dominant forces—from viscous to inertial—but also a deviation from the idealized perfect sphere shape. These changes introduce complexities that the region-specific models, despite their accuracy within their respective domains, were unable to capture. The numerical model, as opposed to the other models, displayed a remarkable flexibility, adjusting to the increasing influences that likely exerted on the raindrop as its diameter expands. This capability to handle the evolving dynamics of raindrops, including the deformation from a perfect spherical shape, is a testament to the model's robustness and applicability across a broad range of scenarios.

8: References

- [1] Doiron, T., 20 Degrees Celsius—A Short History of the Standard Reference Temperature for Industrial Dimensional Measurements, Journal of Research (NIST JRES), National Institute of Standards and Technology, Gaithersburg, MD, [online], 2007, https://tsapps.nist.gov/publication/get_pdf.cfm?pub_id=823211
- [2] “Density of Air.” Wikipedia, Wikimedia Foundation, 20 Oct. 2023, en.wikipedia.org/wiki/Density_of_air.
- [3] “Air - Density vs. Pressure and Temperatures.” Engineering ToolBox, www.engineeringtoolbox.com/air-temperature-pressure-density-d_771.htmlgoogle_vignette.
- [4] “What Everyone Gets Wrong about the Shape of a Raindrop?” Science ABC, 19 Oct. 2023, www.scienceabc.com/pure-sciences/shape-falling-raindrop-pressure-sphere-surface-tension-hydrostatics-aerodynamics-gravity-myth.html.
- [5] Helmenstine, Anne. “The Real Raindrop Shape Is Not a Teardrop.” Science Notes and

Projects, 10 May 2021, sciencenotes.org/the-real-raindrop-shape-is-not-a-teardrop/.

[6] Ross Gunn and Gilbert D. Kinzer. The Terminal Velocity of Fall for Water Droplets in Stagnant Air. *Journal of Meteorology*, vol. 6 (1949), pp. 243-248.

[7] “Dropping the Ball (Slowly).” Stokes’ Law, galileo.phys.virginia.edu/classes/152.mf1i.spring02/Stokes_Law.htm.

[8] “Cannonball Aerodynamic Drag.” ARC, arc.id.au/CannonballDrag.html.

[9] Polezhaev, Yury V., and I.V. Chircov. “Drag Coefficient.” THERMOPEDIA, Begel House Inc., www.thermopedia.com/content/707/.

9: ChatGPT Usage

I used ChatGPT as an assistant throughout my code and a plot helper. After some debugging attempts specifically when trying to plot **Figure 4** and **Figure 5**, I used it for successfully applying the Newton-Raphson method to my Pandas DataFrame.

Additionally, I used ChatGPT to fix up wording I believed was a little messy and choppy in my paper. Specifically in my conclusion, when I was trying to compile everything better and relate the problem back to the sphere problem I addressed at the beginning of the paper, I had trouble establishing a strong argument for it and used ChatGPT to expedite that process.